Evidence for highly anharmonic low-frequency vibrational modes in bulk amorphous $Pd_{40}Cu_{40}P_{20}$

D. J. Safarik and R. B. Schwarz
Material Science and Technology Division, Los Alamos National Laboratory, Los Alamos, New Mexico 87545, USA
(Received 19 June 2009; published 24 September 2009)

We have measured the elastic constants of amorphous $Pd_{40}Cu_{40}P_{20}$ (isotropic, two independent elastic constants), single crystal $Pd_{40}Cu_{40}P_{20}$ (tetragonal, six elastic constants), and single crystal $Pd_{50}Cu_{50}$ (fcc, three elastic constants) over the range $3.9<T<300$ K. The temperature dependences of the shear moduli of *crystalline* $Pd_{40}Cu_{40}P_{20}$ and $Pd_{50}Cu_{50}$ are well described by $C(T)=C(0)-BT^2+\Delta C_{\mathrm{Lat}}(T)$, where BT^2 gives the electronic contribution and $\Delta C_{\mathrm{Lat}}(T)$ is the contribution due to the anharmonicity of the lattice vibrations. The temperature dependence of the shear modulus of *amorphous* $Pd_{40}Cu_{40}P_{20}$ includes an additional contribution, $\Delta C_E(T)$, which becomes dominant for $T<20$ K: $C(T)=C(0)-BT^2+\Delta C_{\mathrm{Lat}}(T)+\Delta C_E(T)$. The $\Delta C_E(T)$ contribution can be explained by the presence of a small number of low-frequency, highly anharmonic vibrational modes, which we characterize as Einstein oscillators with temperature $\theta_E \approx 12$ K and Grüneisen parameter $\gamma_E^{C'} \gg 2$. Theory and computer modeling suggest that these modes involve the collective vibration of stringlike arrays of atoms.

DOI: 10.1103/PhysRevB.80.094109 PACS number(s): 62.20.D−, 62.65.+k, 62.80.+f, 63.20.Ry

I. INTRODUCTION

The elastic constants of metallic glasses have several low-temperature anomalies that are not present in crystalline metals.[1–6] Examples of these anomalies are shown in Fig. 1, which plots the temperature dependence of the ultrasonically measured shear modulus, $\Delta C_{44}/C_{44}=[C_{44}(T)-C_{44}(T_0)]/C_{44}(T_0)$ for two metallic glasses[1,4] and two metal single crystals.[7,8] [$C_{44}(T_0)$ is the value of the shear modulus for $T\rightarrow 0$] In well-annealed crystals such as Cu and V the low-temperature elastic constants can usually be described by $\Delta C_{44}/C_{44}=-bT^2-dT^4$.[8,10] The smooth curves through the Cu and V data in Fig. 1 are best fits using this equation. The two contributions to the temperature dependence arise from thermal excitations of the electrons (the T^2 term) and excitations of the anharmonic lattice vibrations (the T^4 term).[8]

In metallic glasses, the temperature dependence of the elastic constants is markedly different. For $0.1<T<2$ K, the shear modulus *increases* with temperature. Near ~2 K the modulus reaches a maximum value and above ~2 K it decreases monotonically. The peculiar increase in the elastic constants at very low temperatures has also been observed in oxide glasses.[11] Jäckle[12] explained this increase in terms of low-energy excitations that can be modeled as an ensemble of two-level quantum tunneling systems (TLS) having a distribution of energy gaps, Δ, extending down to zero energy.[13,14] Granato[15] later proposed a simple thermodynamic explanation for the elastic softening of a defective *crystal* as it is *cooled* to very low temperatures. Here the defects (interstitials in dumbbell configurations) are also assumed to behave as quantum two-level systems. Both models predict that the effects of the two-level systems vanish at higher temperatures. In metallic glasses, this seems to occur at ~2–3 K.

In the range $4<T<20$ K, the elastic constants of metallic glasses decrease approximately *linearly* with temperature. A linear T dependence has been observed for both C_{44} and for C_{11} not only in metallic glasses, but also in oxide[9] and polymer[16,17] glasses, suggesting that it arises from an intrinsic feature of the amorphous state.

Although the two-level tunneling model has gained acceptance as the plausible explanation for the increase in the elastic constants in the range $0.1<T<2$ K, this model does not seem to explain the linear T dependence observed for $T>4$ K. Several models have been proposed to explain this linear decrease. These models are based on (1) coupling of sound waves to *incoherent* two-level tunneling systems (e.g., incoherent wave functions for the two energy minima assumed in the TLS model);[18] (2) *thermally activated* relaxations between the minima (as opposed to tunneling relaxations);[19] (3) resonant coupling of ultrasonic waves to soft (low-frequency) phonon modes;[20,21] (4) relaxation of the soft modes;[20] and (5) scattering of sound waves by fracton modes.[22]

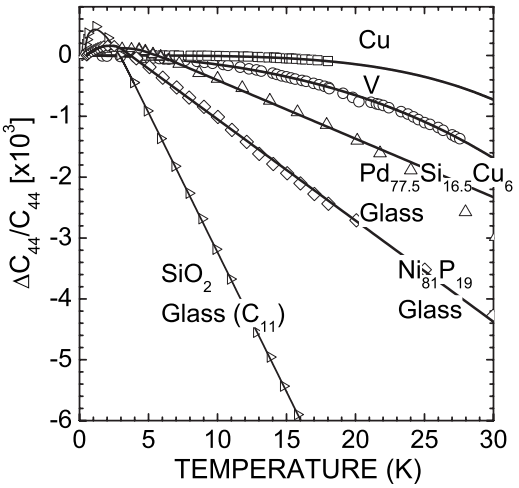

FIG. 1. Relative change in the shear modulus, $\Delta C_{44}/C_{44}=[C_{44}(T)-C_{44}(T_0)]/C_{44}(T_0)$, as a function of temperature for single crystal Cu[7] and V,[8] and for amorphous $Ni_{81}P_{19}$ (Ref. 1) and amorphous $Pd_{77.5}Si_{16.5}Cu_6$.[4] The relative change in the longitudinal modulus, $\Delta C_{11}/C_{11}$, of amorphous SiO_2 (Ref. 9) is also shown. The smooth curves through the Cu and V data are the best fits of $\Delta C_{44}/C_{44}=-bT^2-dT^4$ to the data. The curves through the $Ni_{81}P_{19}$, $Pd_{77.5}Si_{16.5}Cu_6$, and SiO_2 data are lines to guide the eye.

We stated previously that at low temperatures the elastic constants of crystals, such as Cu and V, follow the dependence $-bT^2-dT^4$ without a linear term. We should add here that this is only true for perfect crystals having no lattice defects, or for crystals whose lattice defects are pinned by solutes or other defects. Alers and Zimmerman[7] compared the elastic constants of copper single crystals of two slightly different purities: 99.87% pure and 99.98% pure. Whereas the elastic constants of the lower purity crystal followed the anticipated $\Delta C/C=-bT^2-dT^4$ temperature dependence, the elastic constants of the higher purity crystal decreased *linearly* with temperature in the range $1.5<T<10$ K. This behavior was attributed[7] to the presence of dislocations, which were assumed to be unpinned in the higher purity copper crystal and thus were able to move in response to the applied ultrasonic stress. In the lower purity copper crystal, the dislocations were assumed to be pinned by solutes. Although the dislocation density in these copper crystals was not given, these observations suggest that a density of compliant defects (glissile dislocations in the present case) can modify the T dependence of the elastic constants at low temperatures compared to what is measured in either defect-free crystals or in crystals where the defects are immobilized, for example, via pinning by impurities. A linear T dependence of the elastic constants has also been observed in disordered crystals,[20] quasicrystals,[23] and in irradiated Cu crystals containing a density of isolated interstitial defects in dumbbell configurations.[24] It is somewhat surprising that each of these different types of defects evidently results in a linear T dependence of the elastic constants at low temperatures. This suggests that all these different defects have some common characteristic.

If the defect concentration is relatively low then the contribution of each defect to the temperature dependence of the elastic constants can be considered additive. Thus the moduli of a defective crystal should have three contributions to their temperature dependence: (1) the thermal excitation of the electrons, (2) the excitation of the anharmonic lattice vibrations, and (3) a contribution from the defects. Contributions (1) and (2) together lead to the often observed $\Delta C/C=-bT^2-dT^4$ temperature dependence. Contribution (3) evidently leads to the additional linear T dependence. Because the elastic compliance of each defect can be much larger than that of an equal number of normal-lattice atoms, the defect contributions to the compliance can be dominant within a certain temperature range.

$Pd_{40}Cu_{40}P_{20}$ is the only alloy we know of that can be synthesized both as a bulk metallic glass *and* as a single crystal. This enables us to compare the elastic properties of a bulk metallic glass and a metallic crystal having exactly the same composition. Based on these unique measurements, we propose that the glass contains low-frequency, highly anharmonic vibrational modes not present in the crystal, and it is these modes that are responsible for the linear T dependence of the elastic constants.

Previously[25] we reported the values of the elastic constants of *bulk amorphous* $Pd_{40}Cu_{40}P_{20}$, *single crystal* $Pd_{40}Cu_{40}P_{20}$, and single crystal $Pd_{50}Cu_{50}$ over the range $3.9<T<300$ K. In this paper we analyze the temperature dependence of these data in terms of anharmonic lattice vibrations, using a simplified version of the quasiharmonic model that we develop here. The paper is organized as follows. In Sec. II A, we summarize the quasiharmonic model of Garber and Granato,[26] which gives the *phonon* contribution to the temperature dependence of the elastic constants of a defect-free single crystal (or of a crystal whose dislocations are effectively pinned by solutes). In Sec. II B, we modify Garber and Granato's model to make it useful for the analysis of elastic constant data. We briefly discuss the preparation of the $Pd_{40}Cu_{40}P_{20}$ and $Pd_{50}Cu_{50}$ samples and the measurement of the elastic constants in Sec. III. In Sec. IV we analyze the temperature dependence of our data for single crystal $Pd_{50}Cu_{50}$, single crystal $Pd_{40}Cu_{40}P_{20}$, and amorphous $Pd_{40}Cu_{40}P_{20}$ using our modified version of the quasiharmonic model. To fit the glass data, we are forced to assume that, besides the usual electron and anharmonic phonon contributions to the T dependence, there is an additional contribution from low-frequency and highly anharmonic vibrational modes. We discuss the physical implications of our analysis in Sec. V.

II. TEMPERATURE DEPENDENCE OF THE ELASTIC CONSTANTS: CONTRIBUTION FROM NORMAL ANHARMONIC PHONONS

A. Quasiharmonic model (Garber and Granato, 1975)

If the normal-mode lattice vibrations of a solid were strictly harmonic, there would be no phonon contribution to the thermal expansion, and the phonon contribution to the elastic constants would be independent of temperature. To rigorously account for the anharmonicity of the interatomic potentials is not easy, and approximations are usually made. In the quasiharmonic approximation,[26,27] lattice vibrations are treated as harmonic, but the phonon frequencies ω_a are assumed to depend *explicitly* on the *externally applied* strain ε, and *implicitly* on the *thermal* strain η. Also, the potential energy of the solid is assumed to depend *implicitly* on the *thermal* strain.

Starting from the definition for the isothermal second-order elastic constants, $C^T_{ijkl}=\frac{1}{V}\left(\frac{\partial^2 F}{\partial\varepsilon_{ij}\partial\varepsilon_{kl}}\right)_T$, and the Helmholtz free energy F, Garber and Granato[26] derived the following expression for the phonon contribution to the temperature dependence of C^T_{ijkl}:

$$C^T_{ijkl}(T)=\tilde{C}^0_{ijkl}+\frac{1}{\tilde{V}^0}\sum_{\alpha=1}^{3N}\left\{\left[\gamma^{ij}_\alpha\gamma^{kl}_\alpha-\left(\frac{\partial\gamma^{ij}_\alpha}{\partial\varepsilon_{kl}}\right)_T\right]^0 U^0_\alpha(T)-(\gamma^{ij}_\alpha\gamma^{kl}_\alpha)^0 TC^0_{v,\alpha}(T)\right\}+(\tilde{C}^0_{ijkl}+\tilde{C}^0_{ijklmn})\,\eta(T). \quad (1)$$

The first term on the right, $\tilde{C}^0_{ijkl}$, is the value of the elastic constant at atmospheric pressure and 0 K, *without any lattice vibrations (not even zero point)*. (Here we use a superscript zero to denote atmospheric pressure and 0 K, and the tilde to denote the absence of any lattice vibrations.)

The second term on the right (inside the summation) accounts for the *explicit* dependence of the phonon frequencies

ω_α on the *externally applied* strain ε.[26] The anharmonicity of each vibrational mode is described by the isothermal generalized-mode Grüneisen parameter

$$\gamma_\alpha^{ij} = -\frac{1}{\omega_\alpha}\left(\frac{\partial \omega_\alpha}{\partial \varepsilon_{ij}}\right)_T \tag{2}$$

and its strain derivative $(\frac{\partial \gamma_\alpha^{ij}}{\partial \varepsilon_{kl}})_T$, where T is temperature, α is the vibrational mode index, and ij and kl are the indices of the second-rank strain tensor. The summation is over all $3N$ normal vibrational modes of the solid. $\tilde{V}^0$ is the volume at atmospheric pressure and 0 K, without lattice vibrations, and

$$U_\alpha(T) = \left(\frac{1}{\exp\left[\frac{\hbar\omega_\alpha}{k_B T}\right]-1} + \frac{1}{2}\right)\hbar\omega_\alpha \tag{3}$$

and

$$C_{v,\alpha}(T) = k_B\left(\frac{\hbar\omega_\alpha}{k_B T}\right)^2 \frac{\exp\left[\frac{\hbar\omega_\alpha}{k_B T}\right]}{\left(\exp\left[\frac{\hbar\omega_\alpha}{k_B T}\right]-1\right)^2} \tag{4}$$

are the average internal energy and specific heat, respectively. In Eq. (1), the internal energy and heat capacity both have zero superscripts, indicating that they are evaluated for the vibrational frequencies at atmospheric pressure and 0 K.

The third term in Eq. (1) accounts for the *implicit* dependence of the phonon frequencies and the lattice potential energy on thermal expansion, expressed to first order in η.[26] Here,

$$C_{ijklmn}^T = \left(\frac{\partial C_{ijkl}}{\partial \varepsilon_{mn}}\right)_T \tag{5}$$

is an isothermal third-order elastic constant,

$$\eta(T) = \frac{1}{3\tilde{B}^0\tilde{V}^0}\sum_{\alpha=1}^{3N}\gamma_\alpha^0 U_\alpha^0(T) \tag{6}$$

is the phonon contribution to the linear thermal strain (measured relative to the nonvibrating lattice at 0 K), B is the bulk modulus, and

$$\gamma_\alpha = -\frac{V}{\omega_\alpha}\left(\frac{\partial \omega_\alpha}{\partial V}\right)_T \tag{7}$$

is the scalar-mode Grüneisen parameter. In their derivation, Garber and Granato[26] assumed isotropic thermal expansion and thus the third term in Eq. (1) applies strictly to elastically isotropic or cubic-symmetry materials. As noted by Alers,[8] however, the contribution from expansion is expected to be proportional to thermal strain irrespective of the crystal symmetry.

The elastic constants derived from ultrasonic measurements are *adiabatic*, whereas Eq. (1) gives the *isothermal* elastic constants. For moduli associated with purely deviatoric (volume-conserving) strains, e.g., shear moduli, the adiabatic and isothermal elastic constants have the same value, $C_{ijkl}^S(T) = C_{ijkl}^T(T)$.[26] For any modulus having a *non*deviatoric component, such as C_{11} or the bulk modulus, the adiabatic and isothermal elastic constants are related by[26]

$$C_{ijkl}^S(T) - C_{ijkl}^T(T) = \frac{T}{\tilde{V}^0}\frac{\left[\sum_{\alpha=1}^{3N}\gamma_\alpha^0 C_{v,\alpha}^0(T)\right]^2}{\sum_{\alpha=1}^{3N} C_{v,\alpha}^0(T)}. \tag{8}$$

B. Adaptation of the quasiharmonic model to analyze elastic constant data

Equation (1) gives a rigorous description of the phonon contribution to the temperature dependence of the elastic constants within the quasiharmonic approximation. However, its evaluation requires one to know the frequency and the anharmonicity of all $3N$ normal phonon modes in the solid. Because the frequency spectrum is usually not known (unless one measures the phonon spectrum by, for example, inelastic neutron scattering), and because the anharmonicity of every mode is impossible to obtain, Eq. (1) is not useful for the analysis and interpretation of elastic constant data, at least not in it present form. In this section we derive a simplified version of the quasiharmonic model that is useful for the analysis of data.

The contributions to $C_{ijkl}^T(T)$ arising from zero-point motion can be removed from the sums in Eq. (1) and included in $C_{ijkl}^T(0)$, which is the value of the elastic constant that one would measure at $T=0$ K. The expression for $C_{ijkl}^T(0)$ is

$$C_{ijkl}^T(0) = \tilde{C}_{ijkl}^0 + \frac{1}{\tilde{V}^0}\sum_{\alpha=1}^{3N}\left\{\left[\gamma_\alpha^{ij}\gamma_\alpha^{kl} - \left(\frac{\partial \gamma_\alpha^{ij}}{\partial \varepsilon_{kl}}\right)_T\right]^0 \frac{\hbar\omega_\alpha^0}{2}\right\} + (\tilde{C}_{ijkl}^0 + \tilde{C}_{ijklmn}^0)\frac{1}{3\tilde{B}^0\tilde{V}^0}\sum_{\alpha=1}^{3N}\gamma_\alpha^0\frac{\hbar\omega_\alpha^0}{2}. \tag{9}$$

Using Eq. (9), we can now rewrite Eq. (1) as

$$C_{ijkl}^T(T) = C_{ijkl}^T(0) + \frac{1}{\tilde{V}^0}\sum_{\alpha=1}^{3N}\left\{\left[\gamma_\alpha^{ij}\gamma_\alpha^{kl} - \left(\frac{\partial \gamma_\alpha^{ij}}{\partial \varepsilon_{kl}}\right)_T\right]^0 (U_\alpha^0(T) - U_\alpha^0(0)) - (\gamma_\alpha^{ij}\gamma_\alpha^{kl})^0 T C_{v,\alpha}^0(T)\right\} + (\tilde{C}_{ijkl}^0 + \tilde{C}_{ijklmn}^0)\frac{1}{3\tilde{B}^0\tilde{V}^0}\sum_{\alpha=1}^{3N}\gamma_\alpha^0[U_\alpha^0(T) - U_\alpha^0(0)], \tag{10}$$

where $C_{ijkl}^T(0)$ is the value at 0 K, including the contribution from zero-point energy, and $U_\alpha(T) - U_\alpha(0)$ is the average energy of mode α, not including the zero-point energy:

$$U_\alpha(T) - U_\alpha(0) = \frac{\hbar\omega_\alpha}{\exp\left[\frac{\hbar\omega_\alpha}{k_B T}\right]-1}. \tag{11}$$

Defining *mode-averaged* Grüneisen parameters as

$$\langle \gamma \rangle = \frac{\sum_{\alpha=1}^{3N} \gamma_\alpha C_{v,\alpha}}{\sum_{\alpha=1}^{3N} C_{v,\alpha}}, \tag{12}$$

$$\langle \gamma^{ij}\gamma^{kl} \rangle = \frac{\sum_{\alpha=1}^{3N} \gamma_\alpha^{ij}\gamma_\alpha^{kl} C_{v,\alpha}}{\sum_{\alpha=1}^{3N} C_{v,\alpha}}, \tag{13}$$

and

$$\left\langle \frac{\partial \gamma^{ij}}{\partial \varepsilon_{kl}} \right\rangle_T = \frac{\sum_{\alpha=1}^{3N} \left(\frac{\partial \gamma_\alpha^{ij}}{\partial \varepsilon_{kl}} \right)_T C_{v,\alpha}}{\sum_{\alpha=1}^{3N} C_{v,\alpha}} \tag{14}$$

and assuming that, to a first approximation, these mode-averaged quantities are independent of temperature, we can rewrite Eq. (10) as

$$C_{ijkl}^T(T) = C_{ijkl}^T(0) + \frac{1}{V}\left(\langle \gamma^{ij}\gamma^{kl} \rangle - \left\langle \frac{\partial \gamma^{ij}}{\partial \varepsilon_{kl}} \right\rangle_T + (C_{ijkl} + C_{ijklmm})\frac{\langle \gamma \rangle}{3B} \right) \sum_{\alpha=1}^{3N} (U_\alpha(T) - U_\alpha(0)) - \frac{T}{V}\langle \gamma^{ij}\gamma^{kl} \rangle \sum_{\alpha=1}^{3N} C_{v,\alpha}(T). \tag{15}$$

Notice that in Eq. (15), and for the remainder of this paper, we drop the superscript 0 and the tilde. In doing so we assume that, as a first approximation, the volume, mode-averaged Grüneisen parameters, second- and third-order elastic constants, and vibrational frequencies are independent of temperature, and are not changed by the presence of lattice vibrations.

The sums in Eq. (15) give the lattice contributions to the internal energy (not including zero-point energy),

$$U_{\text{Lat}} = \sum_{\alpha=1}^{3N} [U_\alpha(T) - U_\alpha(0)], \tag{16}$$

and the heat capacity,

$$C_{v,\text{Lat}} = \sum_{\alpha=1}^{3N} C_{v,\alpha}(T). \tag{17}$$

Therefore, within the approximations stated, the T dependence of the elastic constant is given by the relatively simple expression

$$C_{ijkl}^T(T) = C_{ijkl}^T(0) + \frac{1}{V}\left(\langle \gamma^{ij}\gamma^{kl} \rangle - \left\langle \frac{\partial \gamma^{ij}}{\partial \varepsilon_{kl}} \right\rangle_T + (\tilde{C}_{ijkl} + \tilde{C}_{ijklmm})\frac{\langle \gamma \rangle}{3B} \right) U_{\text{Lat}}(T) - \frac{1}{V}\langle \gamma^{ij}\gamma^{kl} \rangle T C_{v,\text{Lat}}(T). \tag{18}$$

The most direct way to determine $C_{v,\text{Lat}}(T)$ is to measure the specific heat. $U_{\text{Lat}}(T)$ then follows from an integration of $C_{v,\text{Lat}}(T)$. Alternatively, one can compute $C_{v,\text{Lat}}(T)$ from the phonon density of states of the solid, $g(\omega)$. The two approaches are equivalent provided the phonon density-of-states data is accurate. For low temperatures, one could also simply use the Debye heat-capacity model. In a Debye solid, $g(\omega) \propto \omega^2$ up to a cutoff frequency ω_D and thus $C_{v,\text{Lat}}$ is proportional to T^3 up to $T \approx \theta_D/10$ (θ_D is the Debye temperature). Therefore, for an electrically insulating Debye solid the elastic constants should vary as $C_{ijkl}^T(T) = C_{ijkl}^T(0)[1 - dT^4]$ for $T < \theta_D/10$, where d is a constant.

Equation (18) gives the T dependence of the elastic constants for an insulating solid, which has contributions only from the excitation of the phonons. To compare with measurements in metallic solids, we must also include the contribution from the thermal excitation of electrons. For temperatures much less than the Fermi temperature, the electronic contribution to the free energy, and hence to the elastic constants, is proportional to T^2,[28]

$$C_{ijkl}^T(T) = C_{ijkl}^T(0) - AT^2 + \frac{1}{V}\left(\langle \gamma^{ij}\gamma^{kl} \rangle - \left\langle \frac{\partial \gamma^{ij}}{\partial \varepsilon_{kl}} \right\rangle_T + (\tilde{C}_{ijkl} + \tilde{C}_{ijklmm})\frac{\langle \gamma \rangle}{3B} \right) U_{\text{Lat}}(T) - \frac{1}{V}\langle \gamma^{ij}\gamma^{kl} \rangle T C_{v,\text{Lat}}(T), \tag{19}$$

where A is a constant. Thus for a metallic Debye solid, the low-temperature elastic constants should vary as $C_{ijkl}^T(T) = C_{ijkl}^T(0)[1 - aT^2 - dT^4]$. In metals with a low density of states at the Fermi level and depending on the shape of the Fermi surface[28] the T^2 term may be negligible at all but the very lowest temperatures, as is the case for copper (Fig. 1). In metals with a high density of states at the Fermi level, however, the T^2 term may dominate up to temperatures of 20 K or more, as is the case for vanadium (Fig. 1).

III. EXPERIMENT

$Pd_{40}Cu_{40}P_{20}$ stock alloy was prepared by melting a mixture of Pd powder, Cu shot, and P chunks in a sealed silica tube. Amorphous $Pd_{40}Cu_{40}P_{20}$ was produced by melting this stock alloy, together with B_2O_3 flux, in another silica tube and then quenching the tube in water. The as-quenched glassy rods, 3 mm in diameter, were cut into 4-mm-long segments by electrodischarge machining (EDM). These cylindrical specimens were used in the elastic constants measurements. Single crystals of $Pd_{40}Cu_{40}P_{20}$ (tetragonal struc-

ture) were grown in silica tubes using the Bridgman technique, starting from the same batch of stock alloy that was used to make the amorphous samples. Parallelepiped-shaped specimens, for use in the elastic constants measurements, were cut from the single-crystal rods using EDM. These specimens had six {100} crystallographic faces and measured $2.2\times1.8\times1.6$ mm^3.

$Pd_{50}Cu_{50}$ stock alloy was prepared by arc melting a mixture of Pd powder (pressed into pellets) and Cu shot in an argon atmosphere. A rod of single crystal $Pd_{50}Cu_{50}$ (disordered fcc solid solution) was grown from this stock alloy using the Bridgman method. Parallelepiped-shaped specimens were cut from the single-crystal rod using EDM. These specimens had six {100} crystallographic faces and measured approximately $5\times4\times3$ mm^3. Further details about the preparation and characterization of the $Pd_{50}Cu_{50}$ and $Pd_{40}Cu_{40}P_{20}$ specimens are presented in Ref. 25.

The elastic constants were measured using resonant ultrasound spectroscopy (RUS). In the RUS technique, the spectrum of mechanical resonances of a sample of well-defined geometry (usually a parallelepiped or cylinder) is measured using piezoelectric transducers. Detailed descriptions of the RUS method have been published.[29–31] In the present measurements, the specimen and the transducers were located inside a liquid He cryostat. The spectrum of resonant frequencies was repeatedly scanned as the sample slowly warmed from 3.9 to ~300 K over a period of several days. The first 30 resonant frequencies of the spectrum were used to determine the two independent elastic constants of the elastically isotropic $Pd_{40}Cu_{40}P_{20}$ glass and the three independent elastic constants of the fcc $Pd_{50}Cu_{50}$ crystal. The first 40 resonant frequencies were used to determine the six independent elastic constants of the tetragonal $Pd_{40}Cu_{40}P_{20}$ crystal. For all three materials, the values of the elastic constants were corrected for thermal expansion. This was done by assuming that the volume thermal-expansion coefficient, β, of each material is isotropic and proportional to the Debye heat capacity, with $\theta_D=300$ K and $\beta\,(\theta_D)=43\times10^{-6}$ K^{-1}.[32]

IV. RESULTS

A. Shear modulus C' of single crystal $Pd_{50}Cu_{50}$

We first deduce the expression for the temperature dependence of the shear modulus C'. We begin by evaluating Eq. (19) for C_{11} and C_{12}. From the definition $C'=(C_{11}-C_{12})/2$, we then obtain

$$C'(T)=C'(0)-AT^2+\frac{1}{V}[\langle(\gamma^{C'})^2\rangle-K_1]U_{\rm Lat}-\frac{1}{V}\langle(\gamma^{C'})^2\rangle TC_{v,\rm Lat}, \tag{20}$$

where

$$\langle(\gamma^{C'})^2\rangle=\frac{1}{2}[\langle(\gamma^1)^2\rangle-\langle\gamma^1\gamma^2\rangle] \tag{21}$$

and

$$K_1=\frac{1}{2}\left[\left\langle\frac{\partial\gamma^1}{\partial\varepsilon_1}\right\rangle_T-\left\langle\frac{\partial\gamma^1}{\partial\varepsilon_2}\right\rangle_T\right]+\frac{1}{2}[C_{11}-C_{12}+C_{111}-C_{123}]\frac{\langle\gamma\rangle}{3B} \tag{22}$$

(notice that we now use Voigt notation, where $11\rightarrow1$, $22\rightarrow2$, $13\rightarrow4$, etc.). Wallace[33] deduced the combination of second- and third-order elastic constants describing the volume-strain dependence of C_{11} and C_{12} for cubic and isotropic solids. Here we have incorporated his results into the expression for K_1. Recall that because C' is a pure shear modulus, the adiabatic and isothermal moduli are equal.

For pure shear deformations, such as those associated with C' and with C_{44}, the *mode-averaged* Grüneisen parameters $\langle\gamma^{C'}\rangle$ and $\langle\gamma^4\rangle$ are equal to zero. This was demonstrated nicely by Mason[34] and Mason and Bateman,[35] who averaged the generalized-mode Grüneisen parameters $\gamma_\alpha^{C'}$ and γ_α^4 for 39 purely longitudinal and purely transverse phonon modes in cubic crystals. However, Eqs. (20) and (21) do not contain the mode averaged of the Grüneisen parameter, but rather the mode average of the Grüneisen parameter *squared*, $\langle(\gamma^{C'})^2\rangle$. Before fitting Eq. (20) to our data, we need to know whether $\langle(\gamma^{C'})^2\rangle$ always equals zero. As we demonstrate in the Appendix, this is not true and $\langle(\gamma^{C'})^2\rangle$ must always be *greater than* zero.

Figure 2(a) shows the temperature dependence of C' for single crystal $Pd_{50}Cu_{50}$. The solid curve is the best fit of Eq. (20) to these data in the range $3.9<T<300$ K.

To fit Eq. (20) to the data, one needs to know $C_{v,\rm Lat}$ and $U_{\rm Lat}$. We have measured the heat capacity at constant *pressure* for single crystal $Pd_{50}Cu_{50}$ in the range $2<T<300$ K. By integrating the $C_{p,\rm Lat}$ data we derived the enthalpy $H_{\rm Lat}$. Because the difference between C_p and C_v is negligible for $T<100$ K (and is usually less than 3% at 300 K), in this range we approximated $C_{v,\rm Lat}(T)\approx C_{p,\rm Lat}(T)$ and $U_{\rm Lat}(T)\approx H_{\rm Lat}(T)$. Using these measured values, Eq. (20) has four adjustable parameters: $C'(0)$, A, $\langle(\gamma^{C'})^2\rangle$, and K_1. By fitting the data in the range $3.9<T<300$ K we obtained $C'(0)=26.43$ GPa, $A=1.11\times10^{-5}$ GPa K^{-2}, $\langle(\gamma^{C'})^2\rangle=2.40$, and $K_1=1.38$. From this value of $\langle(\gamma^{C'})^2\rangle$ we estimate the mode-averaged Grüneisen parameter to be $\sqrt{\langle(\gamma^{C'})^2\rangle}=1.55$.

Figure 2(b) shows the same data and fit as Fig. 2(a) but plotted as $[C'(0)-C'(T)]/C'(0)$ versus temperature and in log-log scale, which emphasizes the behavior at low temperatures. This figure also shows the temperature dependence due to the electrons alone and the phonons alone for $T<40$ K, as deduced from our fit of Eq. (20).

B. Shear modulus C' of single crystal $Pd_{40}Cu_{40}P_{20}$

Figure 3(a) shows C' as a function of temperature for single crystal $Pd_{40}Cu_{40}P_{20}$ and for amorphous $Pd_{40}Cu_{40}P_{20}$. The solid curve through the *crystal* data is the best fit of Eq. (20) for $3.9<T<300$ K, using measured values of $C_{p,\rm Lat}$ (Ref. 36) and $H_{\rm Lat}$. From this fit we obtained the values $C'(0)=41.52$ GPa, $A=1.33\times10^{-5}$ GPa K^{-2}, $\langle(\gamma^{C'})^2\rangle=6.20$, and $K_1=3.25$. Using this value of $\langle(\gamma^{C'})^2\rangle$ we estimate the

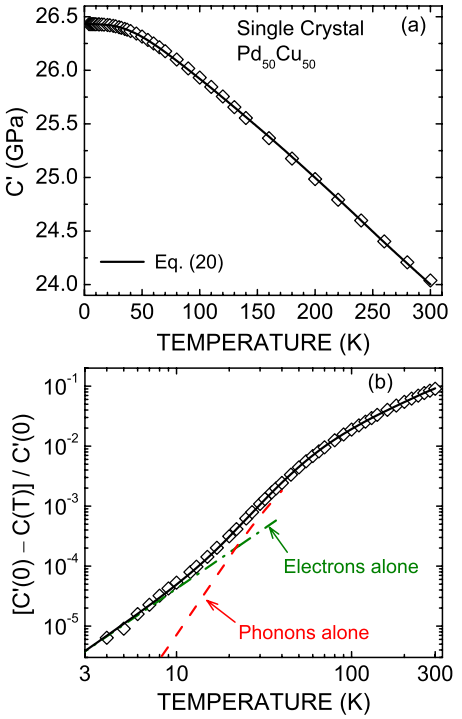

FIG. 2. (Color online) (a) Temperature dependence of the shear modulus C' for single crystal $Pd_{50}Cu_{50}$. The solid curve is the best fit of Eq. (20) over the range $3.9<T<300$ K. (b) Same data as in (a) but plotted as $[C'(0)-C'(T)]/C'(0)$ versus temperature and in log-log scale. The temperature dependence due to the electrons alone and the phonons alone, as determined from fitting Eq. (20), are shown for $T<40$ K.

mode-averaged Grüneisen parameter to be $\sqrt{\langle(\gamma^{C'})^2\rangle}=2.49$. Figure 3(b) shows the crystal data plotted as $[C'(0)-C'(T)]/C'(0)$ vs T and in log-log scale. The dashed curves show the temperature dependence due to the electrons alone and the phonons alone for $T<40$ K, as determined from our fit of Eq. (20).

We have also investigated whether our data for single crystal $Pd_{40}Cu_{40}P_{20}$ can be fitted using approximate values for $C_{v,\mathrm{Lat}}$ and U_{Lat}, given by the Debye model. Figure 4 shows the best fit of Eq. (20) to the C' data, obtained using heat capacities and internal energies *calculated* from the Debye model ($\theta_D=322$ K, as determined calorimetrically). Clearly, using the Debye model, we were unable to fit the data, regardless of the values of $C'(0)$, A, $\langle(\gamma^{C'})^2\rangle$, and K_1. In contrast, using the measured values of $C_{p,\mathrm{Lat}}$ and H_{Lat}, we were able to fit the data nicely over the entire range $3.9<T<300$ K.

We should note that the factor $(C_{11}-C_{12}+C_{111}-C_{123})$ in Eq. (22) applies rigorously to cubic crystals and elastically isotropic solids,[33] which have isotropic thermal expansion. The crystal structure of $Pd_{40}Cu_{40}P_{20}$ has a slight (~6%) tetragonal distortion.[25,37] Because this distortion is small, we treated the $Pd_{40}Cu_{40}P_{20}$ crystal as cubic.

C. Shear modulus of amorphous $Pd_{40}Cu_{40}P_{20}$

We attempted to fit Eq. (20) to the C' vs temperature data for amorphous $Pd_{40}Cu_{40}P_{20}$, using measured values of

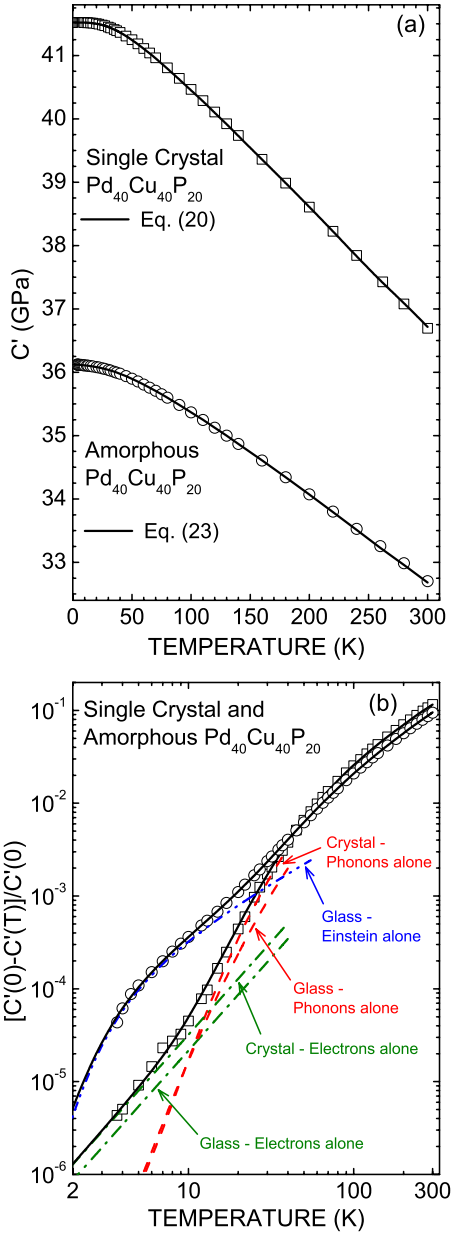

FIG. 3. (Color online) (a) Temperature dependence of the shear modulus C' for single crystal $Pd_{40}Cu_{40}P_{20}$ and amorphous $Pd_{40}Cu_{40}P_{20}$. The solid curve through the crystal data is the best fit of Eq. (20), and the solid curve through the glass data is the best fit of Eq. (23), both using measured values of the heat capacity and internal energy. (b) Same data as in (a) but plotted as $[C'(0)-C'(T)]/C'(0)$ vs T and in log-log scale. The temperature dependence due to the Einstein modes alone, the electrons alone, and the phonons alone, as determined from these fits, are shown for $T<40$ K.

$C_{p,\mathrm{Lat}}(T)$ and $H_{\mathrm{Lat}}(T)$. Although we were able to fit the data in the range $100<T<300$ K, we were unable to fit Eq. (20) to the data below 100 K, irrespective of the values chosen for $C'(0)$, A, $\langle(\gamma^{C'})^2\rangle$, and K_1. This is shown in Fig. 5, where we plot C' vs temperature for amorphous $Pd_{40}Cu_{40}P_{20}$ together with the best fit of Eq. (20) to the data.

All of the glass data between $3.9<T<300$ K could be fitted, however, by assuming that in addition to the usual

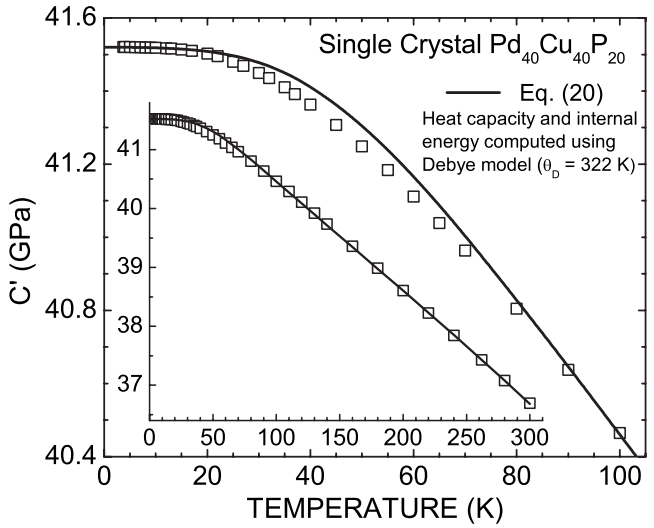

FIG. 4. Temperature dependence of the shear modulus C' for single crystal $Pd_{40}Cu_{40}P_{20}$ in the range $3.9<T<100$ K. Inset: temperature dependence of C' for $3.9<T<300$ K. For both the main figure and the inset, the solid curve is the best fit of Eq. (20) to the data, *using values of the heat capacity and internal energy computed from the Debye model* (θ_D=322 K). We were unable to fit the data in the range $3.9<T<90$ K, regardless of the values chosen for the fitting parameters.

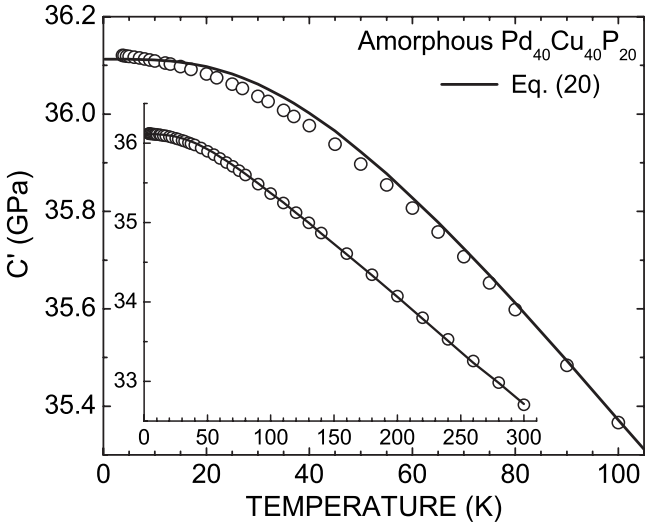

FIG. 5. Temperature dependence of the shear modulus C' for amorphous $Pd_{40}Cu_{40}P_{20}$ in the range $3.9<T<100$ K. Inset: temperature dependence of C' for $3.9<T<300$ K. The solid curve is the best fit of Eq. (20) to the data using *measured* values of heat capacity and internal energy. Equation (20) includes contributions from the electrons and the normal anharmonic phonons but not from the highly anharmonic Einstein modes. We were unable to fit the data in the range $3.9<T<100$ K, regardless of the values chosen for the fitting parameters.

contributions to the T dependence from the electrons and the "normal" anharmonic phonons (with $\sqrt{\langle(\gamma^{C'})^2\rangle}\approx 2$), there is also a contribution from a small number of low-energy vibrational modes with $\sqrt{\langle(\gamma^{C'})^2\rangle}\gg 2$. The justification for this assumption will become clearer in Sec. V D, where we discuss low-energy excitations in glasses. For simplicity, we represent these low-energy, highly anharmonic modes as N_E Einstein oscillators ($N_E\ll 3N$), all with the same frequency ω_E. (As discussed in Sec. V B, our analysis suggests that the number of highly anharmonic modes is indeed small.) Within the quasiharmonic approximation, the vibrational modes of a solid are assumed to be noninteracting and thus their contributions to the free energy, and hence to the elastic constants, are additive. Therefore the temperature dependence of C' for a metal containing a small number[38] of highly anharmonic Einstein modes ($N_E\ll 3N$) is

$$C'(T) = C'(0) - AT^2 + \frac{1}{V}[\langle(\gamma^{C'})^2\rangle - K_1]U_{\mathrm{Lat}} - \frac{1}{V}\langle(\gamma^{C'})^2\rangle TC_{v,\mathrm{Lat}} + \frac{N_E}{V}[\langle(\gamma_E^{C'})^2\rangle - K_{1,E}](U_E(T) - U_E(0)) - \frac{N_E}{V}\langle(\gamma_E^{C'})^2\rangle TC_{v,E}, \quad (23)$$

where the first four terms on the right are identical to Eq. (20), and the last two terms are the contribution of the Einstein modes. The anharmonicity of the Einstein modes is characterized by $\langle(\gamma_E^{C'})^2\rangle$ and $K_{1,E}$, which are defined analogously to $\langle(\gamma^{C'})^2\rangle$ and K_1 [see Eqs. (21) and (22)]. The heat capacity and internal energy, $C_{v,E}$ and $U_E(T)-U_E(0)$, are given by Eqs. (4) and (11), respectively, with $\omega_\alpha=\omega_E$. We should note that if these anharmonic modes are associated with specific defects in a solid, then the defects will also lower the value of $C'(0)$ in addition to changing the temperature dependence of $C'(T)$.

The solid curve through the *glass* data in Fig. 3(a) is the best fit of Eq. (23) for $3.9<T<300$ K, using measured values of $C_{p,\mathrm{Lat}}(T)$ (Ref. 36) and $H_{\mathrm{Lat}}(T)$. From this fit we deduce $C'(0)=36.12$ GPa, $A=7.80\times10^{-6}$ GPa K^{-2}, $\langle(\gamma^{C'})^2\rangle=2.57$ [$\sqrt{\langle(\gamma^{C'})^2\rangle}=1.60$], and $K_1=2.56$ for the normal phonons, and $\theta_E=12.2$ K, $\frac{N_E}{3N}\langle(\gamma_E^{C'})^2\rangle=0.25$, and $\frac{N_E}{3N}K_{1,E}=0.54$ for the Einstein modes. The goodness of this fit does not change appreciably for θ_E in the range $3<\theta_E<15$ K. Figure 3(b) shows the same glass data as Fig. 3(a) but plotted as $[C'(0)-C'(T)]/C'(0)$ versus temperature and in log-log scale. This figure shows the T dependence due to the electrons alone, the phonons alone, and the Einstein modes alone for $T<40$ K, as deduced from our fit of Eq. (23). For temperatures below approximately 20 K, the change in $C'(T)$ is dominated by the Einstein modes.

The fit of Eq. (23) to the glass data does not allow us to decouple $\langle(\gamma_E^{C'})^2\rangle$ or $K_{1,E}$ from $N_E/3N$. However, as discussed in Sec. V B, $N_E/3N\ll 1$. This means that $\sqrt{\langle(\gamma_E^{C'})^2\rangle}\gg 2$ and $K_{1,E}\gg 1$. Therefore, the forgoing analysis suggests that the spectrum of low-energy vibrational excitations in amorphous $Pd_{40}Cu_{40}P_{20}$ alloy consists mostly of normal anharmonic vibrations, with $\sqrt{\langle(\gamma^{C'})^2\rangle}\approx 2$, plus a very small density of low-frequency and highly anharmonic vibrations with $\sqrt{\langle(\gamma_E^{C'})^2\rangle}\gg 2$. The goodness of the fit of Eq. (23) strongly suggests that these latter modes can be modeled as Einstein oscillators.

D. Bulk modulus of amorphous $Pd_{40}Cu_{40}P_{20}$

We begin by deriving the expression for the temperature dependence of the adiabatic bulk modulus $B(T)$. To do so we evaluate Eq. (19) for the isothermal moduli C_{11} and C_{12}, convert these isothermal moduli to adiabatic ones and then apply the definition $B=(C_{11}+2C_{12})/3$. The resulting temperature dependence of the bulk modulus, considering only the contributions from the electrons and the normal anharmonic phonons, is

$$B^S(T) = B(0) - AT^2 + \frac{1}{V}[\langle(\gamma^B)^2\rangle - K_2]U_{\mathrm{Lat}} - \frac{1}{V}[\langle(\gamma^B)^2\rangle - \langle\gamma\rangle^2]TC_{v,\mathrm{Lat}}, \quad (24)$$

where

$$\langle(\gamma^B)^2\rangle = \frac{1}{3}[\langle(\gamma^1)^2\rangle + 2\langle\gamma^1\gamma^2\rangle] \quad (25)$$

and

$$K_2 = \frac{1}{3}\left[\left\langle\frac{\partial\gamma^1}{\partial\varepsilon_1}\right\rangle_T + 2\left\langle\frac{\partial\gamma^1}{\partial\varepsilon_2}\right\rangle_T\right] - \frac{1}{3}[C_{11} + 2C_{12} + C_{111} + 2C_{123} + 6C_{112}]\frac{\langle\gamma\rangle}{3B}. \quad (26)$$

The $\langle\gamma\rangle^2$ term in Eq. (24) arises from the conversion of C_{11} and C_{12} from isothermal to adiabatic, which we accomplished using Eq. (8), plus Eqs. (12) and (17). Equation (26) incorporates the results of Wallace,[33] who deduced the combination of second- and third-order elastic constants describing the volume-strain dependence of C_{11} and C_{12} for cubic and isotropic solids.

Figure 6 shows the temperature dependence of the adiabatic bulk modulus for amorphous $Pd_{40}Cu_{40}P_{20}$. The large scatter in these data (compared to C') results from the inherently lower precision of the RUS method in determining the values of stiffer elastic moduli, particularly when the range of elastic stiffnesses of a solid is large,[25] as is the case for glassy $Pd_{40}Cu_{40}P_{20}$ with $C' \sim 35$ GPa and $B \sim 150$ GPa.

The solid curve in Fig. 6 is the best fit of Eq. (24) to the bulk modulus data in the range $3.9 < T < 300$ K. From this fit we deduced $B(0)=153.49$ GPa, $A=5.51\times10^{-5}$ GPa K^{-2}, $\langle(\gamma^B)^2\rangle - K_2 = 5.38$, and $\langle(\gamma^B)^2\rangle - \langle\gamma\rangle^2 = 5.98$ (we are not able to determine the values of these parameters separately). Also shown is the T dependence due to the electrons alone and the phonons alone for $T<60$ K, as determined from the fit of Eq. (24). Notice that we fitted all of the bulk modulus data in the range $3.9 < T < 300$ K assuming that only the electrons and the normal phonons contribute to the T dependence. In contrast, to fit the shear modulus data it was necessary to assume an additional contribution from a small number of low-energy and highly anharmonic vibrational modes, which we modeled as Einstein oscillators.

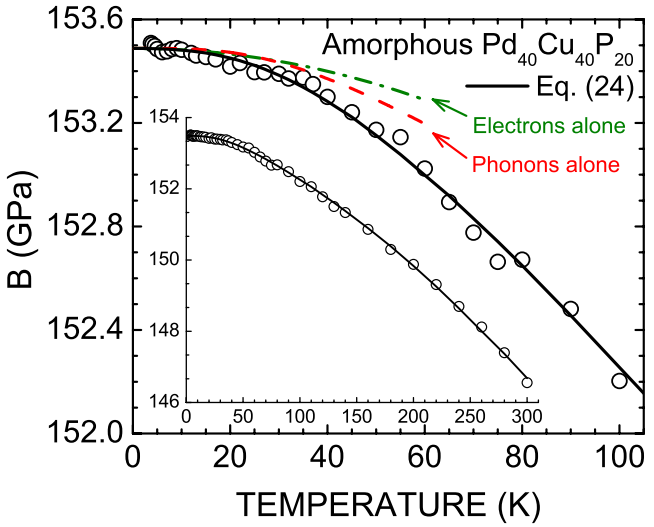

FIG. 6. (Color online) (a) Temperature dependence of the adiabatic bulk modulus B for amorphous $Pd_{40}Cu_{40}P_{20}$ in the range $3.9 < T < 100$ K. Inset: temperature dependence of B for $3.9 < T < 300$ K. The solid curve is the best fit of Eq. (24) to the data using measured values of heat capacity and internal energy. The T dependence due to the electrons alone and the phonons alone, as determined from this fit, is shown for $T<60$ K.

V. DISCUSSION

A. Contribution of the Boson peak to the temperature dependence of the moduli

As shown in Figs. 2, 3, and 6, our elastic constant data are well fitted using *measured* values of $C_{p,\mathrm{Lat}}$ and H_{Lat} to compute the phonon contribution to the temperature dependence. In contrast, in Fig. 4 we showed that the C' data for single crystal $Pd_{40}Cu_{40}P_{20}$ cannot be fitted using values of $C_{v,\mathrm{Lat}}$ and U_{Lat} computed from the *Debye model*. This suggests that the temperature dependence of the elastic constants depends sensitively on the T dependence of the lattice heat capacity and internal energy, and therefore on the particular shape of the phonon density of states.

Previous research has suggested that amorphous solids have low-energy excitations that give characteristic signatures in their low-temperature thermodynamic,[39,40] transport,[40] and acoustic properties.[11] One type of excitation, with energy-level spacings in the range of ~0.1 meV, gives rise to a linear contribution to the heat capacity[40] and a logarithmic contribution to the sound velocity,[11] which are observed at temperatures below ~2 K. These very-low-energy excitations have been modeled as a collection of two-level quantum tunneling systems with a distribution of energy gaps.[13,14] A theory describing the interaction of these two-level systems with ultrasonic waves has been discussed in detail.[12,41] Our elastic constant measurements extended down only to 3.9 K and thus we cannot address these two-level system excitations in amorphous $Pd_{40}Cu_{40}P_{20}$.

A second type of excitation in glasses, with characteristic energy in the ~5 meV range, gives rise to an anomalously large density of vibrational states compared to that predicted by the Debye model, and compared to that measured in crystalline solids of the same composition.[42,43] In oxide glasses,

these vibrational excitations also appear as a broad peak in the low-frequency Raman spectrum.[44] Because the intensity of this Raman peak varies with temperature according to Bose-Einstein statistics, it is often referred to as the "Boson peak."

The presence of the Boson-peak vibrational modes causes the lattice specific heat of glasses to increase more rapidly with temperature than predicted by the Debye model, leading to a pronounced hump in a plot of C_p/T^3 versus T in the range $3<T<20$ K. This hump, however, is not unique to amorphous solids. Indeed, all metallic elements (fcc, bcc, and hcp) show a similar hump in their C_p/T^3 versus T plots, arising from the dispersion of acoustic phonons as the Brillouin-zone boundary is approached, and, in hcp elements, from the excitation of optical phonon branches.[36] Usually, though, the hump is considerably larger for glasses than for crystals, reflecting a larger number of low-frequency vibrational states in the glass than in the crystal.

These additional low-energy vibrational states in glasses should also contribute to the temperature dependence of the elastic constants. This raises the possibility that the linear T dependence of the elastic constants in amorphous $Pd_{40}Cu_{40}P_{20}$, and in other glasses, might be explained naturally in terms of the Boson-peak vibrations. To our knowledge, the connection between the Boson peak modes and the linear T dependence of the moduli in glasses, if any, has not been explored in the literature. We investigated the role of the Boson peak modes in Sec. IV C by using *measured* values of $C_{p,\mathrm{Lat}}$ and H_{Lat}, which already contain the full contribution from the Boson-peak modes, to compute the phonon component of the temperature dependence. Even using these measured values, however, the linear T dependence of the C' data cannot be explained by the phonon and electron contributions alone, without the addition of the Einstein modes. We demonstrate this point in Fig. 5. This strongly suggests that the anomalous T dependence of the elastic constants in the glass observed above ~4 K cannot be explained in terms of the Boson-peak vibrations.

Additional support for this conclusion comes from an analysis of the characteristic energy of the Boson-peak modes. In a previous work[36] we found that the Boson-peak modes in amorphous $Pd_{40}Cu_{40}P_{20}$ give rise to a large hump in C_p/T^3 vs T that is centered at 12 K. By modeling this excess heat capacity (relative to the Debye model) using an array of Einstein oscillators, all with the same frequency, we deduce a characteristic temperature of $\theta_E \approx 60$ K. However, from the analysis in Sec. IV C we deduced a much lower temperature, $\theta_E \approx 12.2$ K. Consequently, the Boson-peak modes, with $\theta_E \sim 60$ K, are simply too high in energy to explain the anomalous temperature dependence that we measure down to 3.9 K in amorphous $Pd_{40}Cu_{40}P_{20}$. All this suggests that *for amorphous* $Pd_{40}Cu_{40}P_{20}$, the anharmonic modes that explain the anomalous temperature dependence of C' have no connection to the vibrational modes that give rise to the Boson peak in its C_p/T^3 vs T plot.

B. Number and anharmonicity of low-energy modes in amorphous $Pd_{40}Cu_{40}P_{20}$

If amorphous $Pd_{40}Cu_{40}P_{20}$ contains low-frequency, highly anharmonic vibrational modes, as suggested by the analysis of our shear modulus data, then these modes should also contribute to the heat capacity at low temperatures. However, we observe no unusual signatures in the heat capacity down to 2 K (the lower limit of our C_p measurements), which is well below the temperature where the anharmonic modes, with $\theta_E = 12.2$ K, become fully excited. One possible explanation is that the number of anharmonic modes is very small and therefore difficult to detect in heat-capacity measurements. An alternative explanation is that the few highly anharmonic modes do not all have the same frequency, as we assumed in fitting the elastic constant data, but rather a distribution of frequencies that make them difficult to distinguish from the background phonon density of states.

If we assume the latter case to be true, then we can estimate the number of highly anharmonic modes. To do so we approximate the density of states for amorphous $Pd_{40}Cu_{40}P_{20}$ using the Debye model, $g(\theta) \propto \theta^2$, where θ is the characteristic temperature. Assuming that all of the vibrational modes with $\theta_E \leq 12.2$ K are highly anharmonic, then by integrating the Debye density of states up to θ_E we estimate the number of these modes as $\frac{N_E}{3N} = (\frac{\theta_E}{\theta_D})^3 = 8.7 \times 10^{-5}$. ($\theta_D = 275$ K, as determined from our low-temperature heat-capacity data.) It is interesting to note that this number is far lower than the density of interstitial-like defects assumed in Granato's interstitialcy model of amorphous solids, which is several percent.[45,46]

Knowing that the number of Einstein modes is small leads us to the conclusion that their anharmonicity is very large, $\sqrt{\langle (\gamma_E^{C'})^2 \rangle} \approx 54$. This result is not unreasonable. Comparably large values of the Grüneisen parameter have been measured for low-energy excitations associated with specific atomic configurations. We can cite three examples: (1) low-frequency, localized "rattler" modes in $Al_{10}V$ ($\theta_E \sim 22$ K) and $Al_{10}V + 0.8\%$ Ga ($\theta_E \sim 8$ K) crystals have Grüneisen parameters of $\gamma \sim 90$;[47] (2) low-frequency ($\theta_E \sim 40$ K) resonant modes associated with ⟨100⟩ split-dumbbell interstitial defects in neutron-irradiated copper have $\gamma^{C'} \sim 40-100$;[24] and (3) tunneling states associated with impurities in alkali halide crystals can have γ values as large as 300.[48]

It is interesting that the highly anharmonic modes do not make an anomalous contribution to the temperature dependence of the bulk modulus, at least not within the precision of our data. Thus although the modes have large anharmonicity in the presence of an applied *shear* stress, $\sqrt{\langle (\gamma_E^{C'})^2 \rangle} \approx 54$, they apparently have normal anharmonicity in the presence of an applied *hydrostatic* stress. An important consequence of this is that the thermal expansion should also show no anomalous temperature dependence, similar to our finding for the bulk modulus.

C. Anelastic relaxations and incoherent tunneling

Thus far we have explained the linear T dependence of C' for amorphous $Pd_{40}Cu_{40}P_{20}$ in terms of a small number of soft ($\theta_E \approx 12$ K) and highly anharmonic $\sqrt{\langle (\gamma_E^{C'})^2 \rangle} \gg 2$) vibrational modes. Our C' data can also be explained, however, in terms of thermally activated anelastic relaxations that occur in the presence of an applied ultrasonic stress. Tiel-

bürger *et al.*[19] developed a model describing the effect of activated relaxations on the acoustic properties of oxide glasses. Their model begins from the standard two-level quantum tunneling model, but assumes that transitions between the two wells can also occur via *thermally activated* hopping over the energy barrier. The model predicts (1) a linear decrease in the modulus with increasing temperature, (2) a logarithmic decrease in the slope $d(\text{modulus})/dT$ with increasing sound wave frequency, and (3) a peak in the internal friction that coincides with the linear T dependence of the modulus.[19] We should point out that to obtain these predictions, Tielbürger *et al.* was forced to assume specific distributions for the model parameters, most notably the number of double wells having a specific asymmetry energy and specific barrier height.

The predictions of Tielbürger's model are consistent with his own data, as well as data available in the literature for the *oxide* glass SiO_2 (Ref. 19 and references therein). Specifically, the SiO_2 data show that the slope $d(\text{modulus})/dT$ varies logarithmically over 7 orders of magnitude of frequency and the internal friction has a peak at ~50 K.

We have compared the predictions of Tielbürger's model to our data for amorphous $Pd_{40}Cu_{40}P_{20}$. The mechanical resonant frequencies of our specimens spanned the range 250–750 kHz and thus the values of C' obtained using the RUS method represent averages over this frequency range. Consequently, we cannot use these data to analyze the frequency dependence of the slope dC'/dT. We have, however, investigated the frequency dependence by determining the slope df/dT for 11 different resonant modes that depend almost entirely (>98%) on C'. From this analysis we detect no frequency dependence of df/dT and hence none for dC'/dT in the range 250–750 kHz.

The only other measurements we know of for the frequency dependence of a metallic glass are those of Bellessa for Pd-Si.[9] These data for Pd-Si indicate a frequency-*independent* slope dC'/dT in the range of 20–400 MHz, which is consistent with our result for $Pd_{40}Cu_{40}P_{20}$. For both $Pd_{40}Cu_{40}P_{20}$ and Pd-Si metallic glasses, the lack of frequency dependence is inconsistent with the prediction of Tielbürger's model. However, it is *consistent* with the anharmonic vibration model that we propose here. The reason is that the relaxation time τ for the anharmonic modes should be small, certainly less than 10^{-9} seconds, and hence $\omega\tau \ll 1$ for all the sound wave frequencies ω used in our measurements. Since $\omega\tau \ll 1$, no relaxation will be observed, and hence df/dT is independent of frequency.

Rau *et al.*[18] suggested a different explanation for the unusual T dependence of the moduli in glasses. They proposed that *incoherent* tunneling (e.g., incoherent wave functions) between the double wells assumed in the TLS model is responsible for the anomaly. The predictions of their incoherent tunneling model[18] are similar to those of the relaxation model, namely, (1) a linear T dependence of the modulus, (2) a slope $d(\text{modulus})/dT$ that varies as the logarithm of the sound wave frequency, and (3) a peak in the T dependence of the internal friction. Thus, just as for the relaxation model, the incoherent tunneling model can explain the data for oxide glasses such SiO_2, B_2O_3, and GeO_2, but it cannot explain the available data for metallic glasses.

D. Atomistic interpretation of low-energy, highly anharmonic vibrations

The large anharmonicity ($\sqrt{\langle(\gamma_E^{C'})^2\rangle} \approx 54$) of the low-energy vibrations suggests that they are associated with specific "defects" in the glass structure, rather than with normal traveling phonons, for which we expect $\gamma \approx 2$. In addition, from their low frequency (~1 meV) we can infer that the vibrating entities have a large mass, a small restoring force, or both. These conclusions lead us to ask the questions: what atomic displacements are involved with these vibrations? Why is the vibrational frequency so small and the anharmonicity so large? Below we discuss these questions, first briefly for oxide glasses and then for metallic glasses.

The oxide glass B_2O_3 contains a large density of vibrational modes with energy ~2.5 meV.[44] The associated atomic displacements consist of rigid librations of several interconnected six-atom boroxyl rings, which are the basic structural units of B_2O_3 formed by alternating boron and oxygen atoms.[44] Glassy SiO_2 also contains a large density of low-frequency (~5 meV) vibrational modes. These vibrations are analogous to those in B_2O_3, involving the rigid librations of interconnected SiO_4 units.[42] Thus for both B_2O_3 and SiO_2, the excess low-energy vibrations are quasilocalized and involve the collective motion of many atoms, and hence are more akin to resonant vibrational modes than to traveling acoustic phonons. However, these 2.5 meV vibrations in B_2O_3 and 5 meV vibrations in SiO_2 do not seem to be responsible for the observed linear T dependence of the elastic constants down to ~4 K. The reason is that these modes are simply too high in energy. Furthermore, it is interesting to note that these modes have normal anharmonicity, e.g., $\gamma \approx 2$, as measured by Raman and neutron scattering.[42,44]

It is unlikely that rigid unit librations, such as in B_2O_3 and SiO_2, exist in metallic glasses such as $Pd_{40}Cu_{40}P_{20}$ since these close packed, nondirectionally bonded glasses lack clearly identifiable structural units, except perhaps for the presence of metallic "cages" surrounding each metalloid atom. However, numerous molecular-dynamics simulations, performed using a variety of different pair-wise interatomic potentials, indicate that metallic glasses have a different type of low-energy excitation, where atoms in stringlike arrays vibrate collectively and at very low frequencies (for example, Refs. 49–51). These stringlike excitations usually occur adjacent to specific defects in the glass structure, namely, regions of excess free volume.[49] The simulations of Laird and Schober[49] suggest that these collective vibrations are composed of up to 50 atoms and have a characteristic vibrational energy of $\sim \theta_D/30$. This agrees with the frequency of the Einstein oscillators we used to explain the temperature dependence of C' in amorphous $Pd_{40}Cu_{40}P_{20}$.

Strings of atoms moving collectively are also found in defective *crystalline* lattices. In neutron-irradiated Cu, for example, each interstitial atom assumes a dumbbell configuration, aligned along a ⟨100⟩ direction, with two Cu atoms trying to occupy the same lattice site. The libration resonant mode of the dummbell interstitial (E_g^1 symmetry) pushes atoms along ⟨110⟩ directions, creating, in effect, four strings.[46,52] The dumbbells and their strings couple readily to

TABLE I. Isothermal generalized-mode Grüneisen parameters associated with C_{11}-, C_{22}-, C'-, and C_{44}-type deformations for sodium chloride. The Grüneisen parameters are computed for 39 purely longitudinal and purely transverse phonon modes using the method of Brugger (Ref. 54) and Mason and Bateman (Ref. 35). The values of the second- and third-order elastic constants for NaCl are (in units of GPa): C_{11}=49.3, C_{12}=12.9, C_{44}=12.78, C_{111}=−880, C_{112}=−57, C_{123}=28.4, C_{144}=25.7, C_{166}=−61.1, and C_{456}=27.1 (Ref. 35).

Mode no.	Propagation direction	Polarization direction	γ_α^1	γ_α^2	$(\gamma_\alpha^2-\gamma_\alpha^1)/2$ $(=\gamma_\alpha^{C'})$	γ_α^4	$\gamma_\alpha^1\gamma_\alpha^2$
1	⟨100⟩	⟨100⟩	7.42	0.45	−3.49	0	3.32
2	⟨100⟩	⟨010⟩	0.46	0.89	0.21	0	0.41
3	⟨100⟩	⟨001⟩	0.46	−1.51	−0.99	0	−0.70
4	⟨010⟩	⟨010⟩	0.45	7.42	3.49	0	3.32
5	⟨001⟩	⟨001⟩	0.45	0.45	0	0	0.20
6	⟨010⟩	⟨100⟩	0.89	0.46	−0.21	0	0.41
7	⟨001⟩	⟨100⟩	0.89	−1.51	−1.20	0	−1.34
8	⟨010⟩	⟨001⟩	−1.51	0.46	0.99	0	−0.70
9	⟨001⟩	⟨010⟩	−1.51	0.89	1.20	0	−1.34
10	⟨011⟩	⟨011⟩	−0.28	2.84	1.56	0	−0.79
11	⟨0-11⟩	⟨0-11⟩	−0.28	2.84	1.56	0	−0.79
12	⟨011⟩	⟨0-11⟩	0.82	4.30	1.74	0	3.52
13	⟨0-11⟩	⟨011⟩	0.82	4.30	1.74	0	3.52
14	⟨011⟩	⟨100⟩	0.89	−0.52	−0.71	0	−0.46
15	⟨0-11⟩	⟨100⟩	0.89	−0.52	−0.71	0	−0.46
16	⟨110⟩	⟨110⟩	2.84	2.84	0	0	8.04
17	⟨1-10⟩	⟨1-10⟩	2.84	2.84	0	0	8.04
18	⟨101⟩	⟨101⟩	2.84	−0.28	−1.56	0.75	−0.79
19	⟨10-1⟩	⟨10-1⟩	2.84	−0.28	−1.56	−0.75	−0.79
20	⟨110⟩	⟨1-10⟩	4.30	4.30	0	0	18.47
21	⟨1-10⟩	⟨110⟩	4.30	4.30	0	0	18.47
22	⟨101⟩	⟨10-1⟩	4.30	0.82	−1.74	0.15	3.52
23	⟨10-1⟩	⟨101⟩	4.30	0.82	−1.74	−0.15	3.52
24	⟨110⟩	⟨001⟩	−0.52	−0.52	0	0	0.27
25	⟨1-10⟩	⟨001⟩	−0.52	−0.52	0	0	0.27
26	⟨101⟩	⟨010⟩	−0.52	0.89	0.71	−1.56	−0.46
27	⟨10-1⟩	⟨010⟩	−0.52	0.89	0.71	1.56	−0.46
28	⟨111⟩	⟨111⟩	1.42	1.42	0	−0.21	2.01
29	⟨1-11⟩	⟨1-11⟩	1.42	1.42	0	−0.21	2.01
30	⟨11-1⟩	⟨11-1⟩	1.42	1.42	0	0.21	2.01
31	⟨1-1-1⟩	⟨1-1-1⟩	1.42	1.42	0	0.21	2.01
32	⟨111⟩	⟨−1-12⟩	1.52	1.52	0	0.55	2.30
33	⟨1-11⟩	⟨−112⟩	1.52	1.52	0	0.55	2.30
34	⟨11-1⟩	⟨−1-1-2⟩	1.52	1.52	0	−0.55	2.30
35	⟨1-1-1⟩	⟨−11-2⟩	1.52	1.52	0	−0.55	2.30
36	⟨111⟩	⟨−110⟩	3.10	3.10	0	0.62	9.61
37	⟨1-11⟩	⟨110⟩	3.10	3.10	0	0.62	9.61
38	⟨11-1⟩	⟨−110⟩	3.10	3.10	0	−0.62	9.61
39	⟨1-1-1⟩	⟨110⟩	3.10	3.10	0	−0.62	9.61
Mode Average, $\langle\gamma_\alpha\rangle=\Sigma\gamma_\alpha/39$			1.58	1.58	0	0	3.13
Mode Average of Square, $\langle(\gamma_\alpha)^2\rangle=\Sigma(\gamma_\alpha)^2/39$			5.85	5.85	1.36	0.23	
$\langle(\gamma_\alpha^{C'})^2\rangle=\frac{1}{2}[\langle(\gamma^1)^2\rangle-\langle\gamma^1\rangle\langle\gamma^2\rangle]=1.36$							

an applied deviatoric strain, thus affecting the values of both C' and C_{44}. The elastic and thermal properties of the dumbbell interstitials have been studied in fcc metals such as Cu by both experiment[24] and computer modeling.[53] Two important conclusions are reached from these studies. First, a distinct feature of the dumbbell interstitial defects is that they have large entropy and large shear compliance. Second, resonant vibrational modes associated with the ⟨100⟩ split-dumbbell interstitial defects in Cu have a low frequency ($\theta_E \sim 40$ K) and huge anharmonicity for both C'-type and C_{44}-type deformations ($\gamma_E^{C'} \sim 40-100$, and comparably large for γ_E^{44}).[24] The low frequency can be explained by the string-like chains of atoms displaced by the vibration of the dumbbell interstitial, which leads to a large effective mass. It is not clear, however, why the resonance vibrational modes associated with the dumbbells are so anharmonic, with $\gamma_E^{C'} \sim 40-100$. Furthermore, it is not known whether the anharmonicity can be ascribed to the motion of the two atoms forming the dumbbell or to the displacements of the strings, since in fcc Cu their motion is intimately coupled.

In contrast to the dumbbells' response to a deviatoric strain, there is no reason to expect the dumbbells in irradiated Cu to couple to a nondeviatoric strain, although we cannot confirm this because bulk modulus data for irradiated Cu is not available.[24]

If chainlike vibrational excitations are present in metallic glasses, as suggested by computer simulations, then based on the above discussion it is likely that these vibrations are highly anharmonic and are thus responsible for the linear T dependence of the shear moduli we measure in amorphous $Pd_{40}Cu_{40}P_{20}$. Thus, the analogy between our results and those for neutron-irradiated Cu cannot be ignored.

Granato[45,46] was the first to see the connection between the strings associated with the dumbbell interstitials in irradiated Cu and the strings now ubiquitous to computer simulation of metallic glasses.[49–51] In his interstitialcy model, Granato proposes that the dynamics of a metallic glass are akin to that of an fcc crystal containing a few percent interstitial defects in dumbbell configurations. As discussed above, a main characteristic of these interstitials is their association with strings of displaced atoms. Our present work supports Granato's interstitialcy model for the glassy state in that we attribute the linear T dependence of C' and C_{44} to the presence of "strings" of atoms in the glass. We differ with this theory, however, in that the number of strings needed to explain the linear T dependence is much smaller than the number of strings assumed in the interstitialcy theory (a few percent). We also differ in the characteristic vibrational energy for these excitations. Whereas our elastic constant measurements suggest the characteristic energy is in the 1 meV range ($\sim \theta_D/30$), the interstitialcy model assumes the characteristic energy is in the 4 meV range ($\sim \theta_D/7$), and assumes further that the string excitations are responsible for the Boson peak in the glass. In contrast, our elastic constant data suggests that the Boson peak has nothing to do with the excitation of the strings.

VI. SUMMARY AND CONCLUSIONS

The temperature dependence of the elastic constants for single crystal $Pd_{50}Cu_{50}$ and $Pd_{40}Cu_{40}P_{20}$ can be well explained using our simplified version of the quasiharmonic model. By fitting this model to our C' data, we estimate the mode-averaged Grüneisen parameter, $\sqrt{\langle(\gamma^{C'})^2\rangle}$, to be 1.55 for $Pd_{50}Cu_{50}$ and 2.49 for $Pd_{40}Cu_{40}P_{20}$.

The temperature dependence of C' for amorphous $Pd_{40}Cu_{40}P_{20}$ can be well explained by an extension of the quasiharmonic model, in which we assume that the vibrational density of states consists mainly of normal vibrations, with $\sqrt{\langle(\gamma^{C'})^2\rangle}=1.60$, plus a small number of low-frequency ($\theta_E \approx 12$ K) and highly anharmonic ($\sqrt{\langle(\gamma_E^{C'})^2\rangle} \approx 54$) vibrational modes, which we model as Einstein oscillators.

The present analysis for amorphous $Pd_{40}Cu_{40}P_{20}$ suggests that the anomalous T dependence observed in our C' data, and the *Boson peak* observed in both the phonon density of states and the heat capacity, arise from *different excitations*. The Boson peak modes alone *cannot* account for the linear contribution to the T dependence, even if we assume that these modes are highly anharmonic. These Boson-peak modes, with characteristic temperature of $\theta \sim 60$ K, are simply too high in energy to explain the linear temperature dependence we measure down to 3.9 K.

Amorphous $Pd_{40}Cu_{40}P_{20}$ appears to have at least three types of low-energy excitations. In order of increasing energy these are: (a) very-low-energy excitations, at a fraction of a meV, which are usually described by tunneling phenomena (these excitations were not addressed in the present work); (b) very-low-frequency and *highly anharmonic* $\sqrt{\langle(\gamma_E^{C'})^2\rangle} \approx 54$) vibrations that can be well represented by Einstein oscillators with $\hbar\omega_E \sim 1$ meV; and (c) normal lattice vibrations ($\sqrt{\langle(\gamma^{C'})^2\rangle}=1.60$). A most notable difference between excitations (b) and (c) is the large anharmonicity of (b).

The Boson peak, which sometimes has been considered a *signature* of the glassy state, seems to be unremarkable, at least in its effect on the elastic properties of a metallic glass. Its ubiquitous presence merely reflects a deviation of the phonon density of states from that predicted by the Debye model. What seems to be a unique characteristic of the glassy state, at least for metallic glasses, is the presence of a small density of low-frequency and highly anharmonic modes. These modes seem to express themselves most strongly in the temperature dependence of the elastic constants at low temperatures.

ACKNOWLEDGMENTS

The Los Alamos National Laboratory Directed Research and Development (LDRD) Program provided financial support for this research.

APPENDIX

Brugger[54] solved the equations of motion for the propagation of long-wavelength plane waves in a homogenously strained solid. From this he derived expressions for the isothermal generalized-mode Grüneisen parameters γ_α^{jj} in terms of the second- and third-order elastic constants. The resulting equations are given in Ref. 54. Using Brugger's results,

Mason[55] deduced expressions for the Grüneisen parameters γ_α^1 and γ_α^4 (corresponding to C_{11}- and C_{44}-type deformations, respectively) for 39 phonon modes. In his analysis, Mason considered one pure longitudinal wave and two pure shear waves propagating along the three independent ⟨100⟩ directions, six ⟨110⟩ directions, and four ⟨111⟩ directions of a cubic crystal, for a total of 39 modes.

Mason and Bateman[35] evaluated these expressions for several cubic crystals using elastic constant data available in the literature. In Table I we reproduce their results for γ_α^1 and γ_α^4 for NaCl. In addition, the table now includes values of γ_α^2 that we calculated using Brugger's equations, as well as the difference $\frac{1}{2}(\gamma_\alpha^2-\gamma_\alpha^1)$ and product $\gamma_\alpha^1\gamma_\alpha^2$. The difference $\frac{1}{2}(\gamma_\alpha^2-\gamma_\alpha^1)$ is equivalent to $\gamma_\alpha^{C'}$, the Grüneisen parameter associated with the shear modulus C'.[34] The mode-averaged values given in Table I are arithmetic means of γ_α^{jj} and $(\gamma_\alpha^{jj})^2$, with equal weight given to each of the 39 modes. This averaging method is equivalent to assuming in Eqs. (12) and (13) that each phonon mode has the same heat capacity (e.g., Dulong and Petit limit).

The average value of $\langle\gamma^1\rangle=1.58$ calculated from these 39 modes agrees well with the measured value of $\langle\gamma^1\rangle=1.54$.[35] Similar agreement is found for other cubic crystals.[35] As shown in the Table, both $\frac{1}{2}\langle\gamma^2-\gamma^1\rangle$ and $\langle\gamma^4\rangle$ are indeed equal to zero, but $\langle(\gamma^{C'})^2\rangle=\frac{1}{4}\langle(\gamma^2-\gamma^1)^2\rangle$ and $\langle(\gamma^4)^2\rangle$ are *greater than zero*. We have also found this to be true for five other cubic crystals that we have investigated. We should point out that the expression for $\langle(\gamma^{C'})^2\rangle$ in Table I is equivalent to Eq. (21), e.g., $\langle(\gamma^{C'})^2\rangle=\frac{1}{4}\langle(\gamma^2-\gamma^1)^2\rangle=\frac{1}{2}[\langle(\gamma^1)^2\rangle-\langle\gamma^1\gamma^2\rangle]$.

The question arises as to whether $\langle\gamma^{C'}\rangle=\langle\gamma^4\rangle=0$ is an artifact due to the small number of phonon modes used for this calculation. Most likely the answer is no. The reason is that the mode average for each *family* of directions (e.g., ⟨100⟩, ⟨110⟩, and ⟨111⟩) equals zero, as can be seen from Table I. This suggests that $\langle\gamma^{C'}\rangle=\langle\gamma^4\rangle=0$ follows from the fact that each atom in the crystal occupies a symmetry center.

[1] G. Bellessa, P. Doussineau, and A. Levelut, J. Physique Lett. **38**, L65 (1977).
[2] G. Bellessa, J. Phys. C **10**, L285 (1977).
[3] G. Bellessa and O. Bethoux, Phys. Lett. **62A**, 125 (1977).
[4] P. Doussineau, J. Phys. Colloq. **42**, 72 (1981).
[5] M. Barmatz and H. S. Chen, Phys. Rev. B **9**, 4073 (1974).
[6] A. K. Raychaudhuri and S. Hunklinger, Z. Phys. B: Condens. Matter **57**, 113 (1984).
[7] G. A. Alers and J. E. Zimmerman, Phys. Rev. **139**, A414 (1965).
[8] G. A. Alers, in *Physical Acoustics*, edited by W. P. Mason (Academic, New York, 1966), Vol. 4, p. 277.
[9] G. Bellessa, Phys. Rev. Lett. **40**, 1456 (1978).
[10] J. Classen, M. Hübner, C. Enss, G. Weiss, and S. Hunklinger, Phys. Rev. B **56**, 8012 (1997).
[11] L. Piché, R. Maynard, S. Hunklinger, and J. Jäckle, Phys. Rev. Lett. **32**, 1426 (1974).
[12] J. Jäckle, Z. Phys. **257**, 212 (1972).
[13] W. A. Phillips, J. Low Temp. Phys. **7**, 351 (1972).
[14] P. W. Anderson, B. I. Halperin, and C. M. Varma, Philos. Mag. **25**, 1 (1972).
[15] A. V. Granato, J. Alloys Compd. **211-212**, 503 (1994).
[16] G. Bellessa, C. Lemercier, and D. Caldemaison, Phys. Lett. **62A**, 127 (1977).
[17] R. Nava and R. Oentrich, J. Alloys Compd. **211-212**, 337 (1994).
[18] S. Rau, C. Enss, S. Hunklinger, P. Neu, and A. Wurger, Phys. Rev. B **52**, 7179 (1995).
[19] D. Tielbürger, R. Merz, R. Ehrenfels, and S. Hunklinger, Phys. Rev. B **45**, 2750 (1992).
[20] D. A. Parshin, Phys. Solid State **36**, 991 (1994).
[21] R. Nava, Phys. Rev. B **49**, 4295 (1994).
[22] A. Jagannathan and R. Orbach, Phys. Rev. B **41**, 3153 (1990).
[23] B. E. White, Jr. and R. O. Pohl, Z. Phys. B **100**, 401 (1996).
[24] J. Holder, A. V. Granato, and L. E. Rehn, Phys. Rev. B **10**, 363 (1974).
[25] D. J. Safarik and R. B. Schwarz, Acta Mater. **55**, 5736 (2007).
[26] J. A. Garber and A. V. Granato, Phys. Rev. B **11**, 3990 (1975).
[27] G. Leibfried, and W. Ludwig, Solid State Phys. **12**, 275 (1961).
[28] B. T. Bernstein, Phys. Rev. **132**, 50 (1963).
[29] A. Migliori, J. L. Sarrao, W. M. Visscher, T. M. Bell, M. Lei, Z. Fisk, and R. G. Leisure, Physica B (Amsterdam) **183**, 1 (1993).
[30] R. G. Leisure and F. A. Willis, J. Phys.: Condens. Matter **9**, 6001 (1997).
[31] R. B. Schwarz and J. F. Vuorinen, J. Alloys Compd. **310**, 243 (2000).
[32] H. S. Chen, J. T. Krause, and E. A. Sigety, J. Non-Cryst. Solids **13**, 321 (1974).
[33] D. C. Wallace, Phys. Rev. **162**, 776 (1967).
[34] W. P. Mason, J. Acoust. Soc. Am. **42**, 253 (1967).
[35] W. P. Mason and T. B. Bateman, J. Acoust. Soc. Am. **40**, 852 (1966).
[36] D. J. Safarik, R. B. Schwarz, and M. F. Hundley, Phys. Rev. Lett. **96**, 195902 (2006).
[37] T. D. Shen, U. Harms, and R. B. Schwarz, Appl. Phys. Lett. **83**, 4512 (2003).
[38] In deriving Eq. (23), we approximated $\Sigma_{\alpha=1}^{3N-N_E}C_{v,\alpha}(T)\approx\Sigma_{\alpha=1}^{3N}C_{v,\alpha}(T)=C_{v,\mathrm{Lat}}$ and $\Sigma_{\alpha=1}^{3N-N_E}[U_\alpha(T)-U_{\alpha,0}]\approx U_{\mathrm{Lat}}$. Analogous approximations were also made for the definitions of $\langle\gamma^{jj}\gamma^{kl}\rangle$ and $\langle\frac{\partial\gamma^{jj}}{\partial\varepsilon_{kl}}\rangle_T$ (contained in K_1) as well. These approximations hold only for $N_E\ll 3N$. As discussed in Sec. V B, our analysis suggests that number of highly anharmonic modes is indeed small.
[39] O. L. Anderson, J. Phys. Chem. Solids **12**, 41 (1959).
[40] R. C. Zeller and R. O. Pohl, Phys. Rev. B **4**, 2029 (1971).
[41] W. A. Phillips, Rep. Prog. Phys. **50**, 1657 (1987).
[42] U. Buchenau, N. Nücker, and A. J. Dianoux, Phys. Rev. Lett. **53**, 2316 (1984).
[43] A. Meyer, J. Wuttke, W. Petry, A. Peker, R. Bormann, G. Coddens, L. Kranich, O. G. Randl, and H. Schober, Phys. Rev. B **53**, 12107 (1996).
[44] G. Simon, B. Hehlen, R. Courtens, E. Longueteau, and R. Vacher, Phys. Rev. Lett. **96**, 105502 (2006).

[45] A. V. Granato, Phys. Rev. Lett. **68**, 974 (1992).
[46] A. V. Granato, J. Non-Cryst. Solids **156-158**, 402 (1993).
[47] G. J. Legg and P. C. Lanchester, J. Phys. F: Met. Phys. **8**, 2125 (1978).
[48] C. R. Case, K. O. Mclean, C. A. Swenson, and G. K. White, in *Thermal Expansion-1971 (Corning)*, Proceedings of the 1971 Thermal Expansion Symposium, edited by M. G. Graham and H. E Hagy (AIP, New York, 1972).
[49] B. B. Laird and H. R. Schober, Phys. Rev. Lett. **66**, 636 (1991).
[50] C. Donati, J. F. Douglas, W. Kob, S. J. Plimpton, P. H. Poole, and S. C. Glotzer, Phys. Rev. Lett. **80**, 2338 (1998).
[51] H. Teichler, Phys. Rev. E **71**, 031505 (2005).
[52] P. H. Dederichs, C. Lehmann, and A. Scholz, Phys. Rev. Lett. **31**, 1130 (1973).
[53] K. Nordlund, Y. Axhkenazy, R. S. Averback, and A. V. Granato, Europhys. Lett. **71**, 625 (2005).
[54] K. Brugger, Phys. Rev. **137**, A1826 (1965).
[55] W. P. Mason, in *Effect of Impurities and Phonon Processes on the Ultrasonic Attenuation of Germanium, Crystal Quartz, and Silicon*, Physical Acoustics: Principles and Methods, edited by W. P. Mason, Vol. 3 (Academic, New York, 1965), pt. B, Chap. 6.